SI Materials and Methods

Cell culture

All gastric cancer cell lines were purchased from the KCLB (Korean Cell Line Bank) at Seoul National University. AGS, MKN-28, MKN-45, NCI-N87, SNU-484, SNU-601, SNU-668, and SNU-719 cells were maintained in Roswell Park Memorial Institute 1640 (RPMI-1640, Corning, NY, USA) supplemented with 10% FBS (GIBCO) and 1% penicillin/streptomycin (pen-strep, Invitrogen, Carlsbad, CA). YCC-6 and YCC-16 cells were maintained in Minimal Essential Medium (MEM, HyClone-Thermo Scientific, South Logan, UT, USA) supplemented with 10% FBS and 1% pen-strep. Hs746T cells were maintained in Dulbecco's Modified Eagle's Medium (DMEM, HyClone-Thermo Scientific, South Logan, UT, USA) supplemented with 10% FBS and 1% pen-strep. All cells were maintained in a humidified environment at 5% CO2 and 37°C.

RNAi-mediated gene knockdown

The ON-TARGET plus SMARTpool for the human ELOVL4 siRNA (L-010269-00), ELOVL5 siRNA (L-009260-01), FADS1 siRNA (L-008210-01) and a nontargeting pool (siNT, D-001810-10) were purchased from Dharmacon (Lafayette, CO, USA). Hs746T and SNU-484 cells were transfected with 20 nM siRNA using Lipofectamine RNAiMAX (Invitrogen) via the reverse-transfection method according to the manufacturer's protocol. Knockdown efficiencies were confirmed using qRT-PCR or western blot analysis.

Generation and validation of the ELOVL5- and FADS1-KO cell lines

CRISPR/Cas9-mediated disruption of the *ELOVL5* and *FADS1* genes was performed using pSpCas9(BB)-2A-GFP (PX458; Addgene #48138) and pSpCas9(BB)-2A-RFP plasmids (1). Guide RNAs (gRNAs) targeting three different sites of the human *ELOVL5* gene (gRNA#1; 5′-GGCTGGGACCAAAATACATGAGG-3′, gRNA#2; 5′-TATACACCACTAAAATCCCCCGG-3′, and gRNA#3; 5′-AGTTGTCTCTACACCCCAAGCGG-3′) and the human *FADS1* gene (gRNA#1; 5′-TTCCCATTGGCCGAGCCTCGTGG-3′, gRNA#2; 5′-ACATCAGCGAGTTCACCCGCCGG-3′, and gRNA#3; 5′-CTCCTAGCCTACCCAGCTCGGGG-3′) were cloned into pSpCas9(BB)-2A-GFP or pSpCas9(BB)-2A-RFP (SI Appendix, Fig. S2 *G and N*). YCC-16 cells were co-transfected with three plasmids targeting each gene using Lipofectamine 3000 reagent (Invitrogen). After 24 hours, single cells positive for both GFP and RFP were isolated using FACS and single-cell clones were obtained. ELOVL5- and FADS1-KO clones were verified by performing

an immunoblot analysis and DNA sequencing of PCR products generated with the primers around the gRNA target sites (*ELOVL5* forward: 5′- CATGTAACAAGGAGCTTCACCTTGTTTGAT-3′, *ELOVL5* reverse: 5′-AATACTTTAATTTTGAATATCATACGAAAC-3′, *FADS1* forward: 5′-AGCCCAGCTGTGAGTTGCCCAAGAC-3′, *FADS1* reverse: 5′- ATCGAGACAGGATGTGACTCCCTCC-3′).

Cell viability and LDH release assays

Cell viability was determined by measuring the cellular ATP levels using the CellTiter-Glo reagent according to the manufacturer's protocol (CellTiter-Glo® 2.0 Assay, G9243, Promega). Cell-free supernatants were collected and assessed using the LDH release assay with a Cytotoxicity Detection kit (11644793001, Roche). The percent of LDH release was calculated according to the manufacturer's instructions.

Lipid peroxidation assay

Lipid peroxidation was determined with flow cytometry using C11 BODIPY 581/591. First, 200,000 cells well seeded in each well of 6-well plates one day before the experiment. To measure the lipid peroxidation levels, cells were treated with RSL3 (1 μM), followed by an incubation with 2.5 μM C11 BODIPY 581/591 at 37°C for 15 min. Cells were then harvested by trypsinization and transferred to a 1.5 ml microfuge tube, pelleted (3000 rpm, 3 min), and resuspended in 0.5 ml of PBS. The cells were analyzed using the 488-nm laser of a flow cytometer (BD FACSCalibur) for excitation, and data were collected from the FL1 detector. A minimum of 10,000 cells were analyzed per condition. Data were analyzed using FlowJo software.

Glutathione assay

On the day before the experiment, Hs746T and NCI-N87 cells were seeded in 6-well plates. After 8 and 12 h of cysteine deprivation, the cells were harvested and lysed in MES buffer. The total intracellular glutathione content was determined using a glutathione assay kit according to the manufacturer's instructions (703002, Cayman Chemical). Glutathione levels were calculated using a glutathione standard curve and normalized to the total protein concentration in each sample.

DPPH radical scavenging assay

The DPPH radical scavenging activities of SC-26196 and CP-24879 were evaluated using a

spectrophotometer. Briefly, 1 ml of freshly prepared 0.1 mM DPPH in ethanol was mixed with different concentrations of SC-26196 and CP-24879. The mixture was incubated in the dark for 30 min. After incubation, the absorbance was measured at 515 nm.

qRT-PCR analysis

Total cellular RNA was extracted using an Easy-spin Total Extraction kit (17221, Intron Biotechnology, Korea) according to the manufacturer's instructions. The RNA concentration of each sample was determined by measuring the absorbance at 260 nm. Two micrograms of RNA from each sample were reverse transcribed into cDNAs using M-MLV reverse transcriptase (M1705, Promega) according to the manufacturer's instructions. Amplified cDNAs were analyzed using a CFX96 TOUCH Real-Time PCR (Bio-Rad) instrument with the following primers: *ELOVL2* (forward), 5′-AGGCTACAACTTACAGTGTCAAG-3′; *ELOVL2* (reverse), 5′-GAGAAATAGTACCACCAAAGCAC-3′; *ELOVL4* (forward), 5′-TCACTGTACGATGTTTACCTTGT-3′; *ELOVL4* (reverse), 5′-GCCAAATGCAGTTAACCCATAG; *ELOVL5* (forward), 5′-AATAAACAGCCATTCTCTTGCC-3′; *ELOVL5* (reverse), 5′-GCCTTCCCATACTCCTGTTAC-3′; *FADS1* (forward), 5′-CAGACATCAACATGCATCCCT-3′; *FADS1* (reverse), 5′-AGAAGTATTTGTGCTGGTGGT-3′; *FADS2* (forward), 5'-TTAACTTCCAGATTGAGCACCA-3'; *FADS2* (reverse), 5'-TTGGCACATAGAGACTTCACC-3'; *ACSL4* (forward), 5′-TCATGTGCTAGAACTGACAGC-3′; *ACSL4* (reverse), 5′-GTACAGTCTCCTTTGCTTCCTT-3′; *β-Actin* (forward), 5′-CTGGCACCCAGCACAATG-3′; and *β-Actin* (reverse), 5′-GCCGATCCACACGGAGTACT-3′.

Lipid analysis using LC-MS/MS

For global lipid profiling, $1x10^7$ cells were rinsed twice with cold PBS and then with cold water. The cellular lipids were extracted by scraping the cells off the dishes into 1 ml of prechilled 80:20 (v/v) methanol:water twice. After clarification by centrifugation, the supernatant was transferred to a new tube, and 2 ml of chloroform and 1 ml of 0.1 M HCl were added. The mixture was cleared by centrifugation. The lipid extracts were dried under nitrogen gas and reconstituted with 250 μl of an isopropanol:acetonitrile:water (2:1:1, v/v/v) solution. For the analysis of PUFAs, PE-(18:0/20:4), and PE-(18:0/22:4), cells were plated in six-well plates. The lipids were extracted in 400 μl of a 40:40:20 acetonitrile:methanol:water solution containing 0.5% formic acid. The extracts were cleared by centrifugation, and the lipids in the supernatant were directly analyzed. [U-$^{13}C_{16}$] Palmitic acid, tridecanoic acid, and PE-(33:1-d7) were used as internal standards. The lipid analysis was conducted using an

ACQUITY UPLC system (Waters, Milford, MA, USA) coupled to a triple TOF™ 5600 mass spectrometer equipped with an electrospray ionization (ESI) source (AB Sciex, Concord, ON, Canada). Chromatographic separation was performed using an Acquity UPLC BEH C18 column (2.1 mm × 100 mm, 1.7 μm; Waters) at 35°C; binary gradient separation was performed at a flow rate of 0.35 ml/min. The injection volume was 5 μl for the negative ion mode. The mobile phases consisted of 10 mM ammonium acetate in water:acetonitrile (60:40 v/v, solvent A) and 10 mM ammonium acetate in isopropanol:acetonitrile (90:10 v/v, solvent B). The steps of the gradient profile used to equilibrate the initial gradient for subsequent runs were 40-65% B from 0-5 min, 65-70% B from 5-12 min, 70-99% B from 12-15 min, 99% B from 15-17 min, 99-40% B from 17-17.1 min, and 40% B from 17.1-20 min. The mass spectrometer was operated in negative ion mode, and data were acquired in the mass range of 80-1500 *m/z* for the analysis of the lipid extracts. Total ion chromatograms were acquired using the following operating parameters: a capillary voltage of -4,500 V, a nebulizer pressure of 50 psi, a drying gas pressure of 60 psi, a curtain gas pressure of 30 psi, a source temperature of 500°C, a declustering potential of -90 eV, a collision energy of -10 eV for single MS, and a collision energy of -45 eV for MS/MS. Data from MS/MS analyses were acquired using automatic fragmentation, in which the five most intense mass peaks were fragmented. Mass accuracy was maintained with an automated calibrant delivery system interfaced to the second inlet of the DuoSpray source. Spectral data were analyzed with MarkerView™ (AB Sciex) to identify peaks, perform alignments, and generate peak tables of *m/z* values and retention times for samples.

DNA methylation

A SureSelectXT Human Methyl-Seq panel (Agilent Technology, Santa Clara, CA, USA) was used for the quantitative analysis of DNA methylation with a HiSeq 2500 Sequencer (Illumina, San Diego, CA, USA). Raw fastq reads were processed using a pipeline including read quality filtering, genomic alignment withBowtie2 to the reference human genome hg19, and methylation calling with Bisulfite Read Mapper, Bismark2. The functional information of variants was annotated using SnpEff4. For the statistical analyses, R (version 3.6.1) packages, including edgeR (Bioconductor), were used. Differentially methylated CpG loci were identified using the calculated logFC values. The methyl-Seq results were deposited in the Sequence Read Archive (SRA) database of NCBI (accession number PRJNA608754).

Classification of GCs

We obtained the gene expression profiles of GC lines using a HumanHT-12 v3.0 Expression BeadChip

array (Illumina; San Diego, CA, USA) and deposited the data into Gene Expression Omnibus (accession ID: GSE146361). GC lines were classified into molecular subtypes using the non-negative matrix factorization clustering method (R package "NMF" version 0.21.0), where we applied subtype-specific gene signatures that were previously defined in primary tumor tissues (2). We calculated stromal and stem-like scores using a single sample GSEA (GenePattern www.genepattern.org) with the previously defined gene sets (2, 3). Mesenchymal and Intestinal GC cell types are representative in vitro surrogates for chemo-refractory and chemo-sensitive GC patients identified by nProfiler 1 Stomach Cancer assay (2).

Dataset S1. Subtype classification, stem-like score, and stromal score of the gastric cancer cell lines used in this study.

Dataset S2. Microarray data of gastric cancer cell lines

Dataset S3. Fold changes in the expression of genes associated with lipid and iron metabolism in mesenchymal-type GCs (Hs746T, SNU-484, SNU-668, and YCC-16) compared with intestinal-type GCs (MKN-45, NCI-N87, SNU-601, and SNU-719) based on the microarray data.

Supplementary Figure Legends

Fig. S1. Mesenchymal-type GCs, but not intestinal-type GCs, are sensitive to ferroptosis upon cysteine/methionine depletion. (A) GSH levels in mesenchymal-type (Hs746T and SNU-484) and intestinal-type (NCI-N87 and SNU-719) GCs cultured in cysteine/methionine-deficient medium. Data are the means ± s.d. (n=3 independent experiments, with ***P < 0.001 according to two-sided Student's t-tests). (B and C) Relative viability (B) and cell death (C) of GCs cultured in cysteine/methionine-deficient medium, as determined using CellTiter-Glo and lactate dehydrogenase (LDH) release assays. Data are the means ± s.d. (n=3 independent experiments, n.s. denotes not significant, *P < 0.05 and ***P < 0.001 according to two-sided Student's t-tests).

Fig. S2. Validation of antibodies against ELOVL5 and FADS1. (A) Relative mRNA expression levels in GCs determined using a microarray analysis. Data are the means ± s.d. (n=3 independent experiments). (B) Levels of the ELOVL5 protein in GCs detected using two ELOVL5 antibodies, as indicated. The asterisk indicates nonspecific bands. (C) Depletion of the *ELOVL5* mRNA in Hs746T and SNU-484 cells was confirmed by the qRT-PCR analysis. Data are the means ± s.d. (n=3 independent experiments). (D and E) ELOVL5 expression levels in mesenchymal-type (YCC-16, Hs746T, and SNU-484) and intestinal-type (SNU-719) cells lacking ELOVL5 with boiling. (F) Western blot analysis using unboiled lysates. (G) Schematic showing guide RNA (gRNA) target sites within exon 3 (E3) and intron 3 of *ELOVL5* used to generate the ELOVL5 KO#1 and KO#2 clones. Notably, gRNA#1 (gR1) was subcloned into pSpCas9(BB)-2A-GFP and gRNA#2 (gR2) and gRNA#3 (gR3) was subcloned into pSpCas9(BB)-2A-RFP. (H) Verification of the ELOVL5-KO cell lines by immunoblotting using boiled lysates. The asterisk indicates nonspecific bands. (I) Western blot analysis using unboiled lysates. (J) FADS1 proteins were detected with various FADS1 antibodies, as indicated. (K) Depletion of the *FADS1* mRNA in Hs746T cells and SNU-484 cells was confirmed by the qRT-PCR analysis. Data are the

means ± s.d. (n=3 independent experiments). (L) Detection of the FADS1 protein, which was depleted by siRNAs in GCs, using a FADS1 antibody (Atlas Antibodies). (M) Nonspecific detection by other FADS1 antibodies from Abcam, Santa Cruz, GTX, and Proteintech was confirmed in FADS1-ablated Hs746T cells. (N) Schematic showing three different guide RNA (gRNA) target sites around exon 1 and intron 1 of *FADS1* used to generate FADS1 KO#1 and KO#2 clones. For this experiment, gRNA#1 (gR1) and gRNA#3 (gR3) were subcloned into pSpCas9(BB)-2A-RFP and gRNA#2 (gR2) was subcloned into pSpCas9(BB)-2A-GFP. (O) Verification of the FADS1-KO cell lines using immunoblotting.

Fig. S3. A heat map of the lipid profiles obtained from the UPLC/QTOF MS spectra of mesenchymal-type and intestinal-type GC cells. Each value in the map is a colored representation of a calculated Z-score. Z-scores were calculated based on the average value of intestinal-type GC cells and its standard deviation as follows: Z-score = [(MS intensity of lipid molecules – average of MS intensity of lipid molecules in intestinal-type GC cells)/standard deviation of MS intensity of lipid molecules in intestinal-type GC cells]. Lipids are presented as the total number of carbon atoms and the total number of double bonds. Lipids with dissimilar MS/MS spectra but identical numbers of carbon atoms and an equal number of double bonds are marked with [a], [b], and [c].

Fig. S4. Depletion of ELOVL5 or FADS1 decreases the sensitivity of cells to ferroptosis. (A-C) Relative viability of Hs746T, SNU-484, and YCC-16 cells treated with RSL3. ELOVL5 and FADS1 were depleted by pool of four different siRNAs (A and B) or four individual siRNAs (C). (D-F) Lipid peroxidation levels in ELOVL5- or FADS1-depleted Hs746T, SNU-484, and YCC-16 cells following RSL3 stimulation for 1 h, as measured using C11 BODIPY 581/591. Data are the means ± s.d. (n=3 independent experiments, with *P < 0.05, **P < 0.01 and ***P < 0.001 according to two-sided Student's t-tests). (G and H) Bar plots showing the ratios of AdA (C22:4) to AA (C20:4) and AA (C20:4) to DGLA (C20:3) in ELOVL5- and FADS1-depleted YCC-16 (G) and Hs746T cells (H). Levels of PUFAs and PE in ELOVL5- and FADS1-depleted YCC-16 (G) and Hs746T cells (H) determined using LC-MS/MS. Intensities were normalized to the cellular protein level. Data are the means ± s.d. (n=5 independent experiments), with *P < 0.05, **P < 0.01 and ***P < 0.001 according to a two-sided Student's test (n.s. denotes not significant).

Fig. S5. The FADS2 inhibitor (SC-26196) shows no antioxidant activity, whereas the FADS1/2 inhibitor (CP-24879) possesses antioxidant activity at high concentrations. DPPH scavenging activity of FADS

inhibitors at various concentrations (SC-26196 and CP-24879). Data are the means ± s.d. (n=3 independent experiments).

Fig. S6. Exogenous AA supplementation promotes ferroptosis in intestinal-type GCs. (A and B) Relative viability of GCs treated with 2.5 μM AA (A and B) and AA-d8, (B) for 16 h, followed by treatment with RSL3 for 24 h. Data are the means ± s.d. (n=3 independent experiments), with **P < 0.01 and ***P < 0.01 according to two-sided Student's tests. (C) Lipid peroxidation levels in NCI-N87 cells pretreated with 2.5 μM PUFAs (linoleic acid, LA; arachidonic acid-d8, AA-d8) for 16 h and treated with RSL3 for 1 h. Data are the means ± s.d. (n=3 independent experiments), with ***P < 0.01 according to two-sided Student's tests. (D and E) Cell viability and LDH release from NCI-N87 cells cultured in cysteine/methionine-deficient medium in the presence and absence of AA and Fer-1. Data are the means ± s.d. (n=3 independent experiments, n.s. denotes not significant, ***P < 0.001 according to two-sided Student's t-tests).

Fig. S7. The expression of the *ELOVL5* and *FADS1* genes is inversely correlated with DNA methylation. (A-C) *ELOVL5*, *FADS1*, and *ACSL4* mRNA expression and methylation in all cancer cell types (n = 1192). The red boxes indicate a group of GCs. Data were generated from Project Achilles - DepMap (https://depmap.org/portal/achilles/). Scatter plots showing inverse correlations between the mRNA expression of the indicated genes and DNA methylation at their promoter regions. Red dots indicate each GC line, and Pearson's correlation coefficients and P-values are shown in the graphs.

Fig. S8. Downregulation of ELOVL4 alleviates ferroptosis in YCC-16 cells. (A) Relative viability of ELOVL4-depleted GCs treated with RSL3. (B and C) Relative viability (B) and cell death (C) of ELOVL4-depleted YCC-16 cells. (D) Lipid peroxidation levels in ELOVL4-depleted YCC-16 cells following RSL3 stimulation for 1 h, as measured using C11 BODIPY 581/591. Data are the means ± s.d. (n=3 independent experiments, with ***P < 0.001 according to two-sided Student's t-tests).

1. D. Bunina *et al.*, Genomic Rewiring of SOX2 Chromatin Interaction Network during Differentiation of ESCs to Postmitotic Neurons. *Cell Syst* **10**, 480-494.e488 (2020).
2. J.-H. Cheong *et al.*, Predictive test for chemotherapy response in resectable gastric cancer: a multi-cohort, retrospective analysis. *The Lancet Oncology* **19**, 629-638 (2018).
3. K. Yoshihara *et al.*, Inferring tumour purity and stromal and immune cell admixture from expression data. *Nat Commun* **4**, 2612-2612 (2013).

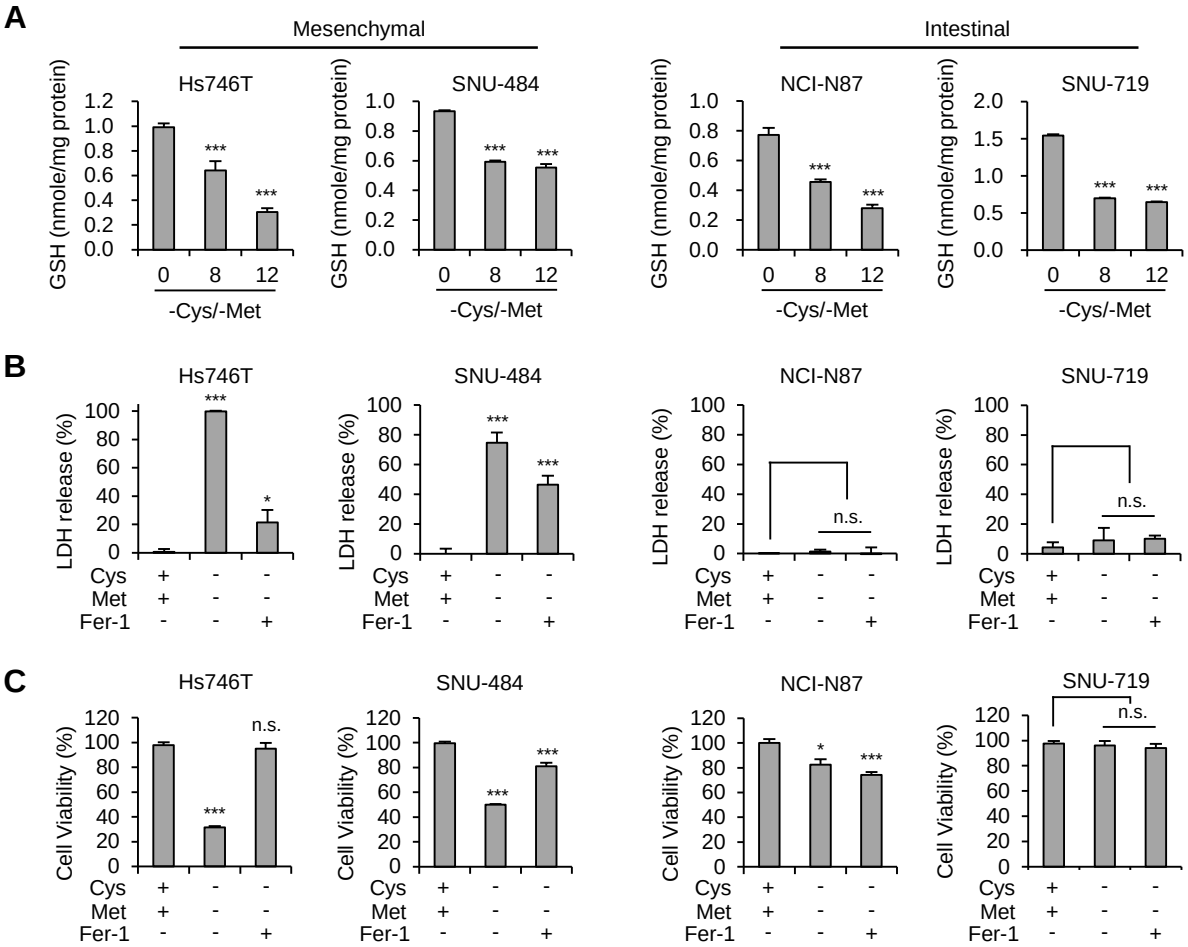
A
Mesenchymal
Intestinal
Hs746T
SNU-484
NCI-N87
SNU-719
GSH (nmole/mg protein)
0 8 12
-Cys/-Met
B
LDH release (%)
n.s.
C
Cell Viability (%)
Cys
Met
Fer-1

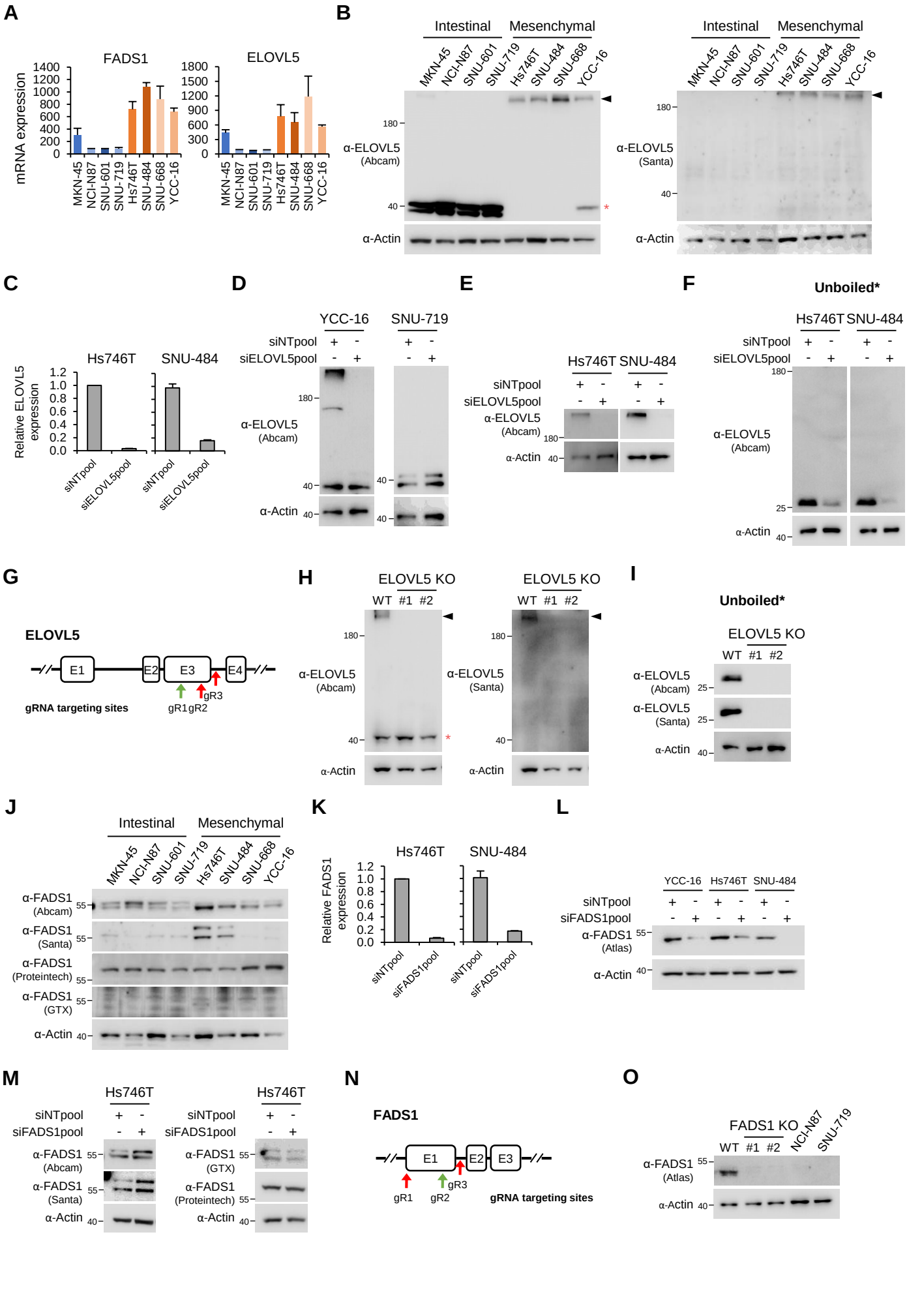
A
FADS1
ELOVL5
mRNA expression
MKN-45
NCI-N87
SNU-601
SNU-719
Hs746T
SNU-484
SNU-668
YCC-16
B
Intestinal
Mesenchymal
α-ELOVL5 (Abcam)
α-ELOVL5 (Santa)
α-Actin
C
Hs746T
SNU-484
Relative ELOVL5 expression
siNTpool
siELOVL5pool
D
YCC-16
SNU-719
E
F
Unboiled*
G
ELOVL5
E1
E2
E3
E4
gRNA targeting sites
gR1
gR2
gR3
H
ELOVL5 KO
WT
#1
#2
I
J
α-FADS1 (Abcam)
α-FADS1 (Santa)
α-FADS1 (Proteintech)
α-FADS1 (GTX)
K
Relative FADS1 expression
siFADS1pool
L
α-FADS1 (Atlas)
M
N
FADS1
O
FADS1 KO

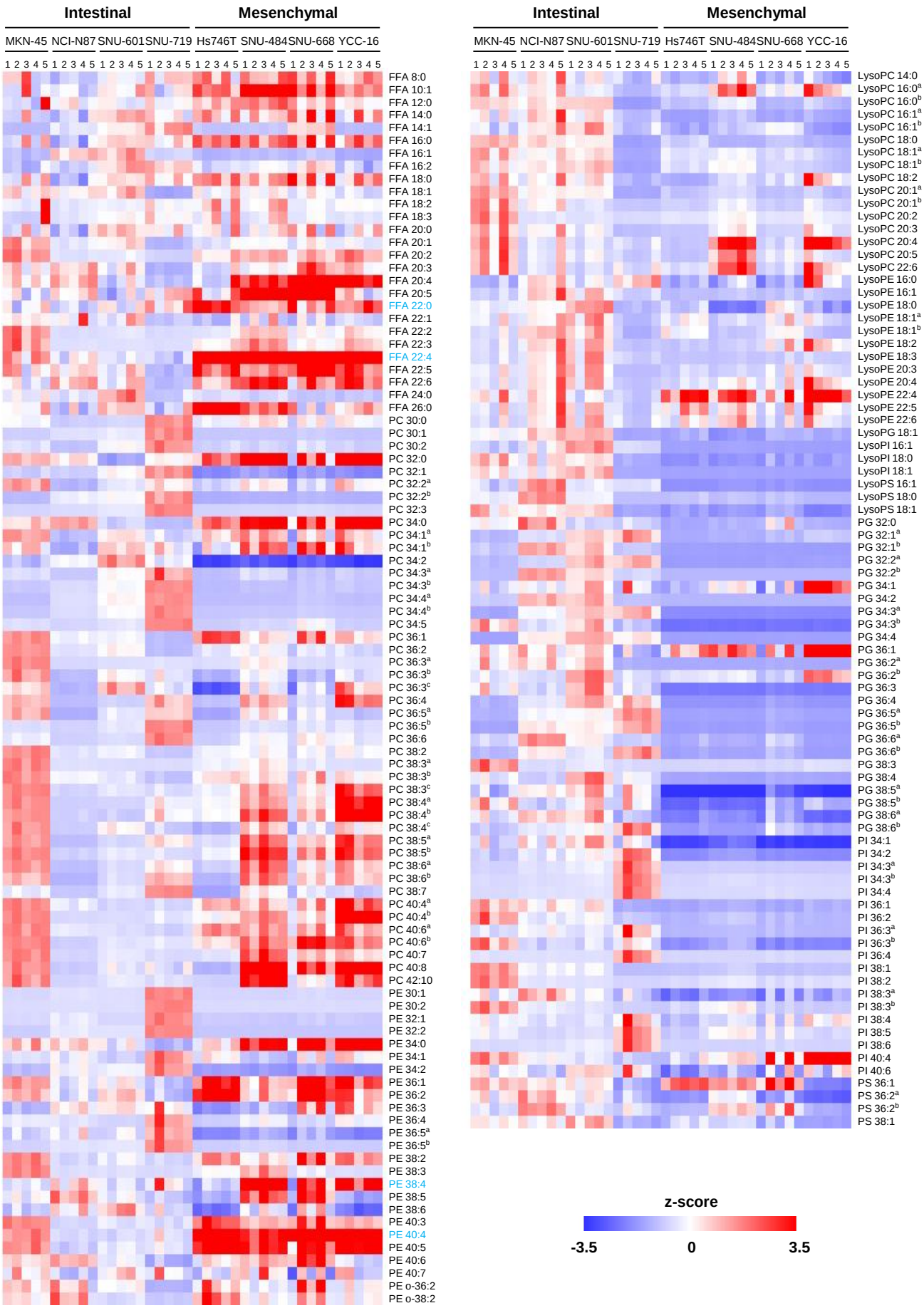
Intestinal
Mesenchymal
MKN-45
NCI-N87
SNU-601
SNU-719
Hs746T
SNU-484
SNU-668
YCC-16
1 2 3 4 5
FFA 8:0
FFA 10:1
FFA 12:0
FFA 14:0
FFA 14:1
FFA 16:0
FFA 16:1
FFA 16:2
FFA 18:0
FFA 18:1
FFA 18:2
FFA 18:3
FFA 20:0
FFA 20:1
FFA 20:2
FFA 20:3
FFA 20:4
FFA 20:5
FFA 22:0
FFA 22:1
FFA 22:2
FFA 22:3
FFA 22:4
FFA 22:5
FFA 22:6
FFA 24:0
FFA 26:0
PC 30:0
PC 30:1
PC 30:2
PC 32:0
PC 32:1
PC 32:2a
PC 32:2b
PC 32:3
PC 34:0
PC 34:1a
PC 34:1b
PC 34:2
PC 34:3a
PC 34:3b
PC 34:4a
PC 34:4b
PC 34:5
PC 36:1
PC 36:2
PC 36:3a
PC 36:3b
PC 36:3c
PC 36:4
PC 36:5a
PC 36:5b
PC 36:6
PC 38:2
PC 38:3a
PC 38:3b
PC 38:3c
PC 38:4a
PC 38:4b
PC 38:4c
PC 38:5a
PC 38:5b
PC 38:6a
PC 38:6b
PC 38:7
PC 40:4a
PC 40:4b
PC 40:6a
PC 40:6b
PC 40:7
PC 40:8
PC 42:10
PE 30:1
PE 30:2
PE 32:1
PE 32:2
PE 34:0
PE 34:1
PE 34:2
PE 36:1
PE 36:2
PE 36:3
PE 36:4
PE 36:5a
PE 36:5b
PE 38:2
PE 38:3
PE 38:4
PE 38:5
PE 38:6
PE 40:3
PE 40:4
PE 40:5
PE 40:6
PE 40:7
PE o-36:2
PE o-38:2
LysoPC 14:0
LysoPC 16:0a
LysoPC 16:0b
LysoPC 16:1a
LysoPC 16:1b
LysoPC 18:0
LysoPC 18:1a
LysoPC 18:1b
LysoPC 18:2
LysoPC 20:1a
LysoPC 20:1b
LysoPC 20:2
LysoPC 20:3
LysoPC 20:4
LysoPC 20:5
LysoPC 22:6
LysoPE 16:0
LysoPE 16:1
LysoPE 18:0
LysoPE 18:1a
LysoPE 18:1b
LysoPE 18:2
LysoPE 18:3
LysoPE 20:3
LysoPE 20:4
LysoPE 22:4
LysoPE 22:5
LysoPE 22:6
LysoPG 18:1
LysoPI 16:1
LysoPI 18:0
LysoPI 18:1
LysoPS 16:1
LysoPS 18:0
LysoPS 18:1
PG 32:0
PG 32:1a
PG 32:1b
PG 32:2a
PG 32:2b
PG 34:1
PG 34:2
PG 34:3a
PG 34:3b
PG 34:4
PG 36:1
PG 36:2a
PG 36:2b
PG 36:3
PG 36:4
PG 36:5a
PG 36:5b
PG 36:6a
PG 36:6b
PG 38:3
PG 38:4
PG 38:5a
PG 38:5b
PG 38:6a
PG 38:6b
PI 34:1
PI 34:2
PI 34:3a
PI 34:3b
PI 34:4
PI 36:1
PI 36:2
PI 36:3a
PI 36:3b
PI 36:4
PI 38:1
PI 38:2
PI 38:3a
PI 38:3b
PI 38:4
PI 38:5
PI 38:6
PI 40:4
PI 40:6
PS 36:1
PS 36:2a
PS 36:2b
PS 38:1
z-score
-3.5
0
3.5

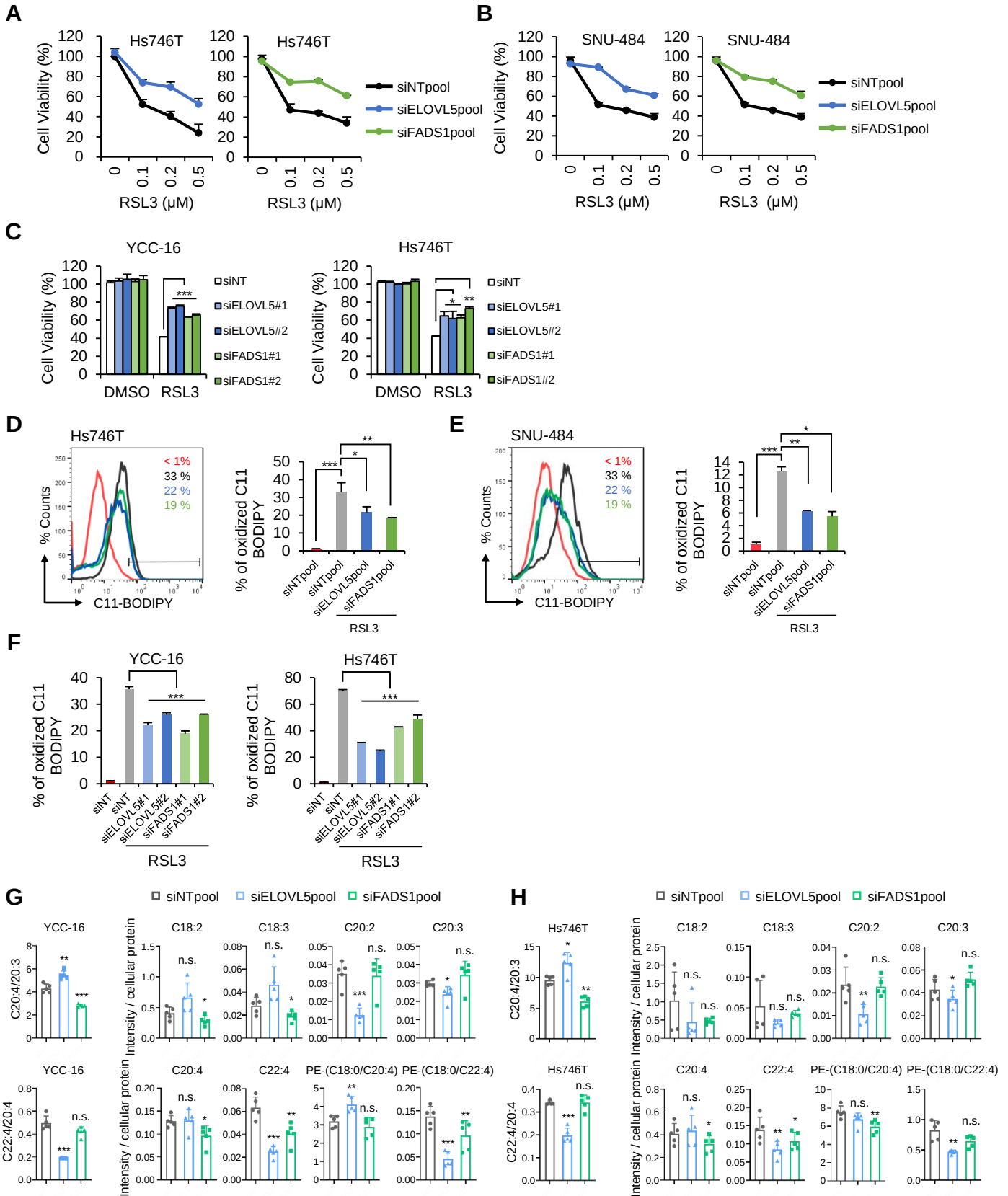
A
Hs746T
Cell Viability (%)
RSL3 (μM)
siNTpool
siELOVL5pool
siFADS1pool
B
SNU-484
C
YCC-16
Hs746T
DMSO
RSL3
siNT
siELOVL5#1
siELOVL5#2
siFADS1#1
siFADS1#2
D
Hs746T
% Counts
C11-BODIPY
< 1%
33 %
22 %
19 %
% of oxidized C11 BODIPY
RSL3
E
SNU-484
F
YCC-16
Hs746T
G
siNTpool
siELOVL5pool
siFADS1pool
C20:4/20:3
C22:4/20:4
Intensity / cellular protein
C18:2
C18:3
C20:2
C20:3
C20:4
C22:4
PE-(C18:0/C20:4)
PE-(C18:0/C22:4)
n.s.
H
Hs746T

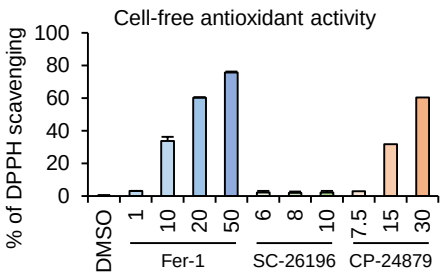
Cell-free antioxidant activity
% of DPPH scavenging
100
80
60
40
20
0
DMSO
1
10
20
50
6
8
10
7.5
15
30
Fer-1
SC-26196
CP-24879

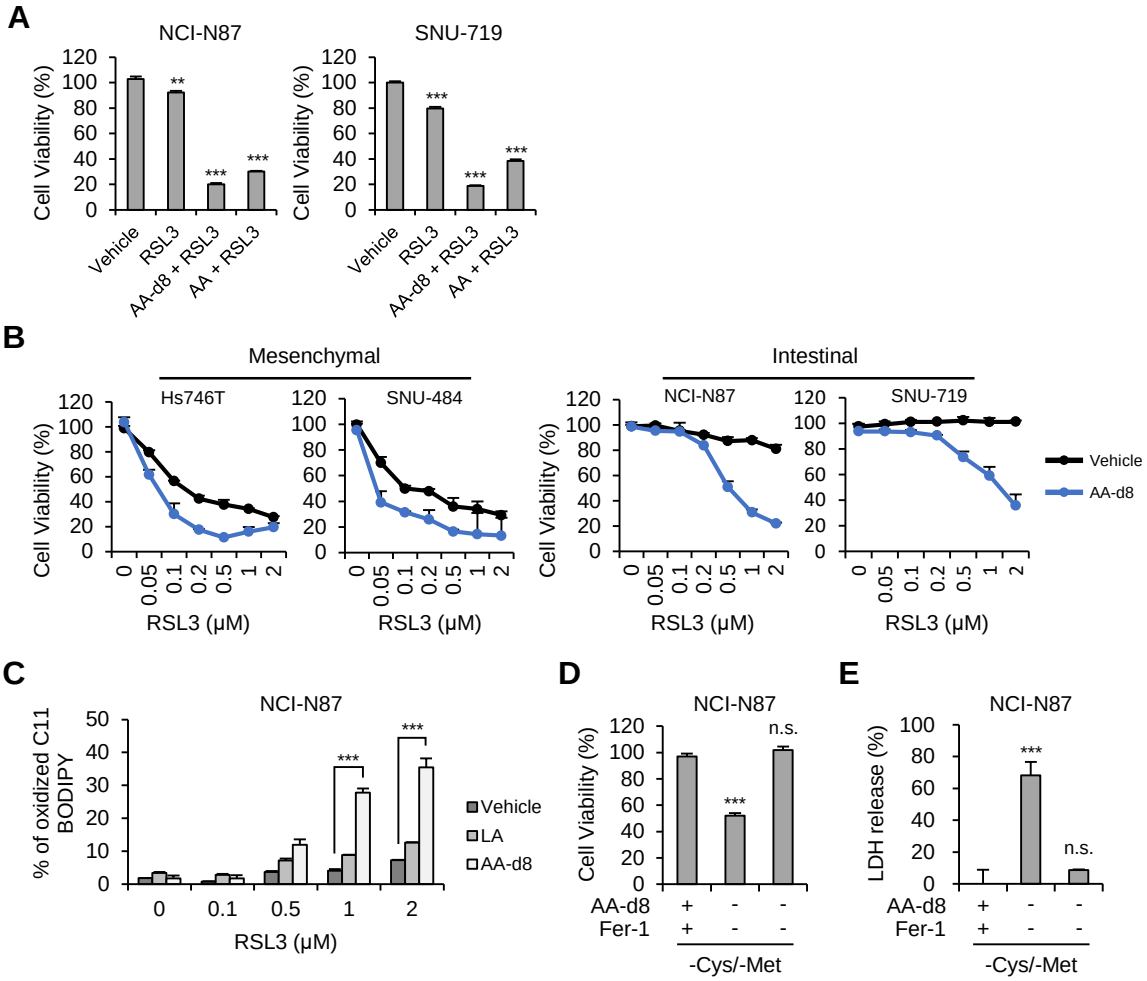
A
NCI-N87
SNU-719
Cell Viability (%)
Vehicle
RSL3
AA-d8 + RSL3
AA + RSL3
B
Mesenchymal
Intestinal
Hs746T
SNU-484
NCI-N87
SNU-719
RSL3 (μM)
Vehicle
AA-d8
C
NCI-N87
% of oxidized C11 BODIPY
Vehicle
LA
AA-d8
RSL3 (μM)
D
NCI-N87
Cell Viability (%)
n.s.
AA-d8
Fer-1
-Cys/-Met
E
NCI-N87
LDH release (%)
n.s.
AA-d8
Fer-1
-Cys/-Met

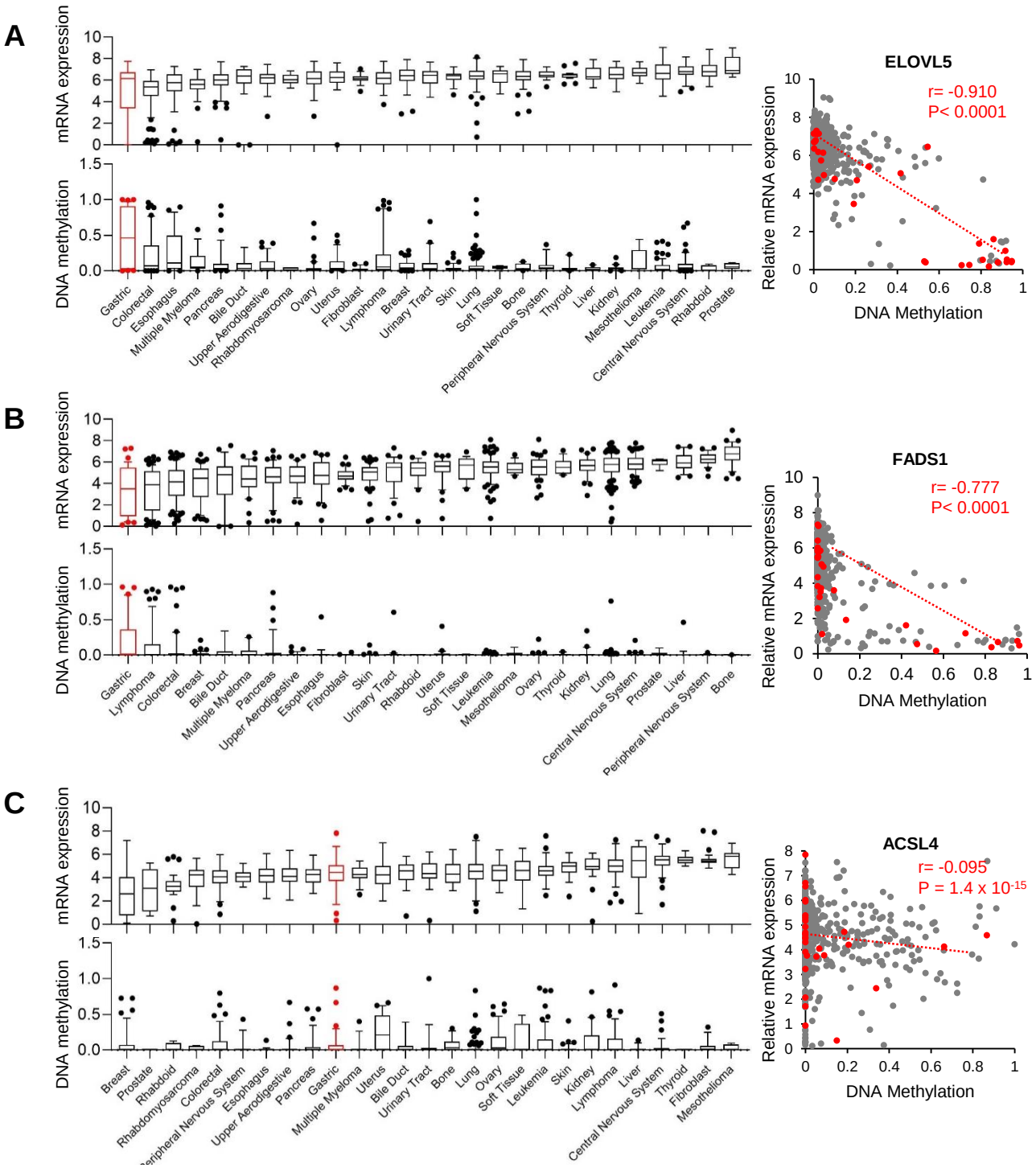
A
mRNA expression
DNA methylation
Gastric
Colorectal
Esophagus
Multiple Myeloma
Pancreas
Bile Duct
Upper Aerodigestive
Rhabdomyosarcoma
Ovary
Uterus
Fibroblast
Lymphoma
Breast
Urinary Tract
Skin
Lung
Soft Tissue
Bone
Peripheral Nervous System
Thyroid
Liver
Kidney
Mesothelioma
Leukemia
Central Nervous System
Rhabdoid
Prostate
ELOVL5
r= -0.910
P< 0.0001
Relative mRNA expression
DNA Methylation
B
mRNA expression
DNA methylation
Gastric
Lymphoma
Colorectal
Breast
Bile Duct
Multiple Myeloma
Pancreas
Upper Aerodigestive
Esophagus
Fibroblast
Skin
Urinary Tract
Rhabdoid
Uterus
Soft Tissue
Leukemia
Mesothelioma
Ovary
Thyroid
Kidney
Lung
Central Nervous System
Prostate
Liver
Peripheral Nervous System
Bone
FADS1
r= -0.777
P< 0.0001
Relative mRNA expression
DNA Methylation
C
mRNA expression
DNA methylation
Breast
Prostate
Rhabdoid
Rhabdomyosarcoma
Colorectal
Peripheral Nervous System
Esophagus
Upper Aerodigestive
Pancreas
Gastric
Multiple Myeloma
Uterus
Bile Duct
Urinary Tract
Bone
Lung
Ovary
Soft Tissue
Leukemia
Skin
Kidney
Lymphoma
Liver
Central Nervous System
Thyroid
Fibroblast
Mesothelioma
ACSL4
r= -0.095
P = 1.4 x 10-15
Relative mRNA expression
DNA Methylation

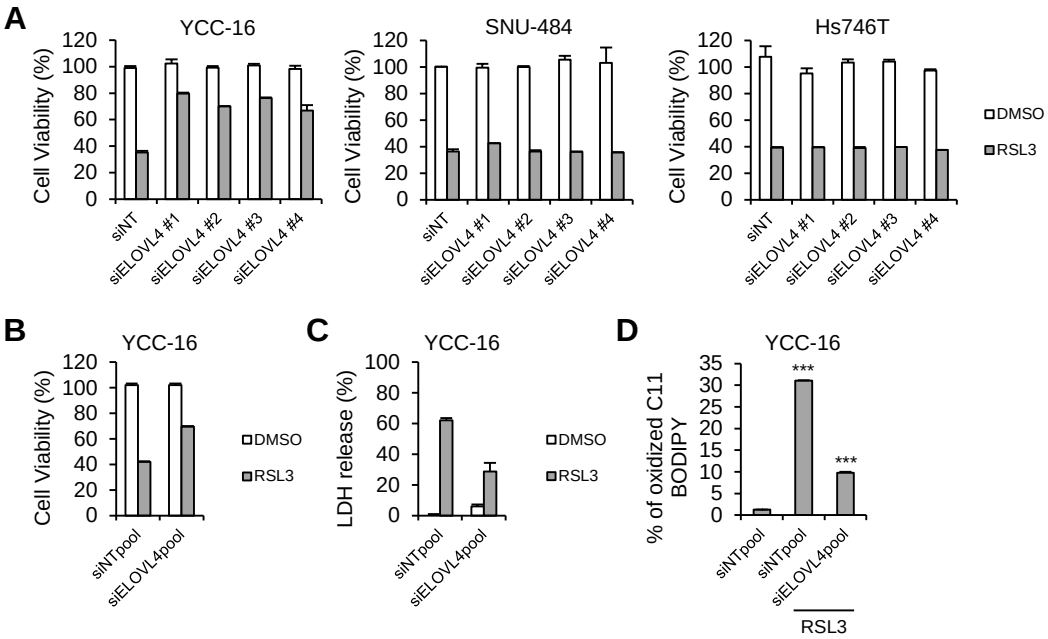
A
YCC-16
SNU-484
Hs746T
Cell Viability (%)
120
100
80
60
40
20
0
siNT
siELOVL4 #1
siELOVL4 #2
siELOVL4 #3
siELOVL4 #4
DMSO
RSL3

B
YCC-16
Cell Viability (%)
120
100
80
60
40
20
0
siNTpool
siELOVL4pool
DMSO
RSL3

C
YCC-16
LDH release (%)
100
80
60
40
20
0
siNTpool
siELOVL4pool
DMSO
RSL3

D
YCC-16
% of oxidized C11 BODIPY
35
30
25
20
15
10
5
0
***
***
siNTpool
siNTpool
siELOVL4pool
RSL3